

Features of the Transport Properties of Thermoelectric Nanocomposites Based on a Matrix from BiSbTe_{1.5}Se_{1.5} Medium-Entropy Alloy and Carbon-Nanotube Filler

O. N. Ivanov^{a,b,*}, M. N. Yapryntsev^{a,c}, A. E. Vasiliev^{a,b}, N. R. Memetov^d, and V. V. Khovailo^{a,c}

^a National Research Technological University Moscow Institute of Steel and Alloys, Moscow, Russia

^b Belgorod State Technological University, Belgorod, Russia

^c Belgorod State University, Belgorod, Russia

^d Tambov State Technical University, Tambov, Russia

*e-mail: Ivanov.Oleg@bsu.edu.ru

Received December 29, 2021; revised January 16, 2022; accepted January 16, 2022

Abstract—For the first time, thermoelectric nanocomposites consisting of a BiSbTe_{1.5}Se_{1.5} medium-entropy alloy (nanocomposite matrix) and “Taunit-M”, CNT carbon nanotubes (nanocomposite filler) are obtained. All BiSbTe_{1.5}Se_{1.5} + xCNT nanocomposites with different filler contents ($x = 0, 0.05, 0.1, 0.5, 1.0, 1.5,$ and 2.0 wt %), obtained by spark plasma sintering of the initial powders of the matrix material and filler, consist of micron-sized filler inclusions formed from clusters of nanotubes. The inclusions themselves are randomly distributed within the polycrystalline matrix. In the temperature range of 290–500 K, the transport properties (electrical resistivity and total thermal conductivity, including the electronic and phonon contributions, as well as the contribution of bipolar thermal conductivity) of the nanocomposites with various filler contents are studied. It is established that the introduction of CNTs into the matrix leads to a qualitative change in the type of electrical conductivity from “metallic” (electrical resistance increases with temperature), characteristic of the nanocomposite matrix, to “semiconductor” (resistance decreases with temperature), characteristic of nanocomposites. The observed “semiconductor” behavior of the electrical conductivity is characteristic of electrically inhomogeneous systems, in which current transfer is determined by the movement of electrons through the interfaces between the inhomogeneities. For all nanocomposites with different filler contents, the temperature dependences of the total thermal conductivity are qualitatively similar. At low temperatures, they are determined by the phonon contribution; at high temperatures, by the bipolar-thermal-conductivity contribution; the electronic contribution manifests itself at all temperatures, but it gradually decreases with increasing x . The minimum thermal conductivity is observed for the nanocomposite with $x = 0.5$ at % CNT.

DOI: 10.1134/S2635167622030077

INTRODUCTION

Carbon nanotubes (CNT) are an important class of carbon nanomaterials. The thermoelectric properties of CNTs are rather moderate (according to the data of review [1], the thermoelectric figure of merit of CNTs, depending on their type and production method, varies from 0.0017 to 0.12, i.e., is very low), which is mainly due to their high thermal conductivity and low Seebeck coefficient. Thus, in thin films consisting of single-walled CNTs, the values of the total thermal conductivity and Seebeck coefficient measured at room temperature are ~ 9.8 $\mu\text{V/K}$ and ~ 38 W/m K , respectively. Due to the low thermoelectric figure of merit, CNTs are not currently considered as an individual thermoelectric material that can find commercial use. Nevertheless, CNTs are widely used in the creation of thermoelectric nanocomposites. In such nanocomposites, CNTs are a filler that can signifi-

cantly improve some thermoelectric properties of the nanocomposite matrix through the following mechanisms:

(i) scattering of electrons and phonons at inhomogeneities, which affects both the electrical and thermal conductivity of the composite;

(ii) the effect of energy filtering of electrons during their tunneling through inhomogeneous matrix/filler interfaces, leading to an increase in the Seebeck coefficient.

It follows from the analysis of published data that the following compounds were used as a matrix in the creation of thermoelectric nanocomposites: Bi₂(Se, Te)₃ [2], Bi₂Te₃ [3], Bi_{0.4}Sb_{1.6}Te₃ [4], MgAgSb [5], Cu₂S [6], Ni_{0.05}Mo₃Sb_{5.4}Te_{1.6} [7], Ce_{0.14}La_{0.06}Co₂Fe₂Sb₁₂ [8].

The overall effect of introducing CNTs into all thermoelectric matrices listed above is a significant

decrease in their thermal conductivity, which leads to a corresponding increase in the thermoelectric figure of merit. For example, the minimum value of the lattice thermal conductivity of the Bi_2Te_3 matrix when single-walled CNTs are introduced into it with a concentration of 0.5 vol % decreases from ~ 1 to ~ 0.25 W/m K [3]. This fact indicates that the CNT filler forms effective scattering centers for phonons. Improvement in the properties of thermoelectric nanocomposites is largely determined by correct choice of the matrix. In addition to the materials listed above, used as a matrix of thermoelectric nanocomposites, other materials are promising for use as matrices, in particular high- and medium-entropy alloys. The development of such alloys is a new strategy in materials science aimed at improving the thermoelectric figure of merit of materials [9–11]. High-entropy alloys usually include solid solutions consisting of at least five different elements with a molar ratio of 5–35% each. They tend to occupy the same site in the crystal lattice, which, accordingly, ensures the maximum entropy of mixing (in medium-entropy alloys, the number of different elements is 3 or 4). In high- and medium-entropy thermoelectric materials, the lattice thermal conductivity can be greatly reduced due to crystal-lattice distortions.

The purpose of this work is to obtain nanocomposites based on a matrix from a medium-entropy alloy $\text{BiSbTe}_{1.5}\text{Se}_{1.5}$ and filler from CNTs and the study of the features of their transport (electrical resistivity and total thermal conductivity) properties.

EXPERIMENTAL

In carrying out the work, $\text{BiSbTe}_{1.5}\text{Se}_{1.5} + x\text{CNT}$ nanocomposites were obtained with a different content of CNTs ($x = 0, 0.05, 0.1, 0.5, 1.5,$ and 2.0 wt %). When obtaining nanocomposites, we used the initial $\text{BiSbTe}_{1.5}\text{Se}_{1.5}$ and CNTs powders, taken in the corresponding required x ratio. For synthesis of the $\text{BiSbTe}_{1.5}\text{Se}_{1.5}$ compound, we used the method of self-propagating high-temperature synthesis (SHS) [14]. Chemically pure Bi, Sb, Se, and Te powders, taken in a stoichiometric ratio, were thoroughly mixed in a vibratory mill for 1.5 h, after which cylinders ~ 18 mm in diameter and ~ 25 mm in height were compacted from the resulting mixture using cold uniaxial pressing. The cylinders (4 pieces) were loaded into a quartz tube, # evacuated with a fore-vacuum pump (to prevent oxidation during SHS) and heated with a propane burner, which made it possible to provide rapid and local heating of the tube to $\sim 1300^\circ\text{C}$. After the SHS process was initiated by such heating, the burner was turned off. The SHS process was fully completed within ~ 5 s, after which the tube was cooled to room temperature. To obtain a homogeneous initial $\text{BiSbTe}_{1.5}\text{Se}_{1.5}$ powder, the resulting cakes were ground in a vibratory mill for 1.5 h.

Carbon nanotubes “Taunit-M”, which are filamentous formations of polycrystalline graphite of cylindrical shape with an internal channel, were obtained by chemical vapor deposition by the pyrolysis of a propane-butane mixture on a Co-Mo/ Al_2O_3 / Mg_2O_3 catalyst. The catalyst was sputtered onto a substrate disk 1 m in diameter. The disk with the catalyst was placed in the reactor, the reactor was sealed, after which oxygen was displaced from it by supplying argon to the reaction space. Simultaneously with the supply of argon, heating was turned on. When the temperature in the reaction zone reached 650°C and oxygen was completely displaced, the argon supply was stopped and a propane-butane mixture was fed into the reaction zone. The synthesis time was 1 h, after which the supply of the propane-butane mixture was stopped, the heating was turned off, and the supply of argon to the reaction zone was started. After the reactor cooled down to a temperature of less than 60°C , the reactor was opened and the disk-substrate with CNTs was removed.

To obtain $\text{BiSbTe}_{1.5}\text{Se}_{1.5} + x\text{CNT}$ nanocomposites with various x , initial $\text{BiSbTe}_{1.5}\text{Se}_{1.5}$ and CNTs powders were mixed in a ball mill with agate balls 10 mm in diameter for 30 min, then the resulting mixture of powders was subjected to spark plasma sintering (SPS-25/10 system) at a pressure of 40 MPa and a temperature of 673 K for 15 min. As a result of sintering, cylinders with a diameter of 20 mm and a height of 15 mm were obtained. To study the thermoelectric properties of $\text{BiSbTe}_{1.5}\text{Se}_{1.5} + x\text{CNT}$ nanocomposites, samples were cut from cylinders in the form of rectangular bars with dimensions of $2 \times 2 \times 10$ mm and in the form of a disc with a diameter of 10 mm and height of 2 mm.

To study the features of the crystal structure, phase and elemental composition, and microstructure of the developed nanocomposites, we used X-ray phase analysis (Rigaku SmartLab X-ray powder diffractometer) and scanning electron microscopy (SEM) (Quanta 600F microscope), including using the electron backscatter diffraction (EBSD) method and energy dispersive X-ray spectroscopy (EDX). A ZEM-3 setup was used to measure the electrical resistivity ρ by the four-probe method and the Seebeck coefficient S by the differential method on samples in the form of bars. The full thermal conductivity k was measured on disc-shaped samples by the laser-flash method on a TC-1200H setup. The quantities ρ , S and k were used to calculate the thermoelectric figure of merit ZT according to the Ioffe formula $ZT = S^2T/k\rho$, where T is the absolute temperature.

RESULTS AND DISCUSSION

The X-ray diffraction pattern of the initial $\text{BiSbTe}_{1.5}\text{Se}_{1.5}$ powder, which is the matrix of the developed nanocomposites, is shown in Fig. 1. The powder is single-phase with a hexagonal crystal struc-

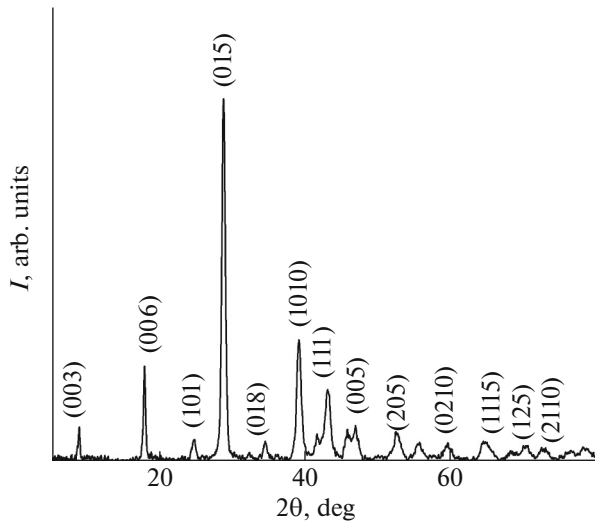


Fig. 1. X-ray diffraction pattern of $\text{BiSbTe}_{1.5}\text{Se}_{1.5}$ powder used as a matrix in preparing the $\text{BiSbTe}_{1.5}\text{Se}_{1.5} + x\text{CNT}$ nanocomposite.

ture (space Group $R\bar{3}m$) and the unit-cell parameters $a = b = 4.182$, $c = 29.752$ Å.

The CNTs used as nanocomposite fillers were cylindrical filaments several microns long and ~ 50 nm thick; in the powder, according to scanning-electron-microscopy data (Fig. 2), they were mainly represented as clusters of a large number of intertwining nanotubes.

The formation of the “matrix-filler” microstructure characteristic of composites in $\text{BiSbTe}_{1.5}\text{Se}_{1.5} + x\text{CNT}$ nanocomposites was confirmed by EBSD analysis-images obtained from their polished surfaces. As an example, such an image for a nanocomposite with $x = 0.5$ wt % CNTs is shown in Fig. 3, where filler inclusions are visible as black areas randomly distributed in a light-gray matrix. The typical size of the inclusions was several microns, and the maximum size did not exceed ~ 10 μm. An EBSD image of one of the CNT inclusions for the same nanocomposite is shown in the inset to Fig. 3. An inclusion ~ 10 μm in size has an irregular shape and a pronounced internal structure. To determine the features of the microstructure of the matrix and the inclusion of the filler of the nanocomposites, SEM images of the cleavage of their surface were obtained. In Fig. 4a, one of the CNT inclusions embedded in the $\text{BiSbTe}_{1.5}\text{Se}_{1.5}$ matrix, is given for the nanocomposite with $x = 0.5$ wt % CNTs. It can be seen that the matrix is polycrystalline with randomly oriented lamellar grains of micron size. In turn, the filler inclusion consists of CNT clusters (Fig. 4b). Thus, in contrast to the previously studied thermoelectric nanocomposites with CNTs, in which nanotubes were uniformly distributed in the matrix volume, in the nanocomposites under study, nano-

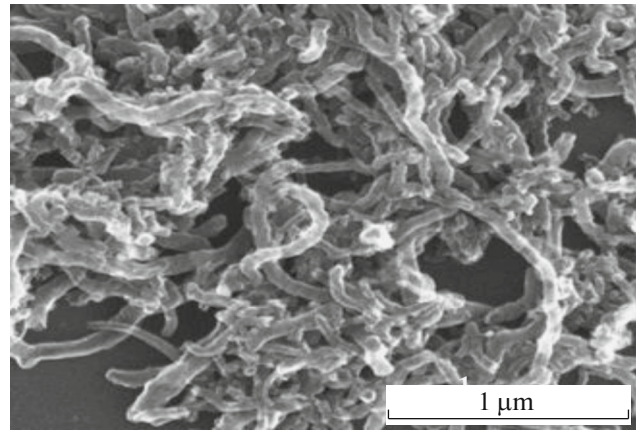


Fig. 2. SEM image of CNTs used as a filler in the preparation of $\text{BiSbTe}_{1.5}\text{Se}_{1.5} + x\text{CNT}$ nanocomposite.

tubes form separate inclusions with pronounced boundaries and consist of a large number of nanotubes, i.e., there is a significantly inhomogeneous distribution of CNTs in the $\text{BiSbTe}_{1.5}\text{Se}_{1.5}$ matrix.

To determine the exact elemental composition of both the inclusions themselves and the matrix material using the EDX method, we studied the distribution of Bi, Te, Sb, Se, and C along the line crossing one of the inclusions, the EBSD image of which is shown in Fig. 5a. By means of analysis of the element scanning profiles, it was found that the matrix corresponds only to the $\text{BiSbTe}_{1.5}\text{Se}_{1.5}$ compound, i.e., no carbon is observed in the matrix. However, in the inclusions, in addition to carbon corresponding to the nanotubes, Te is observed; during sintering, Te penetrates into the

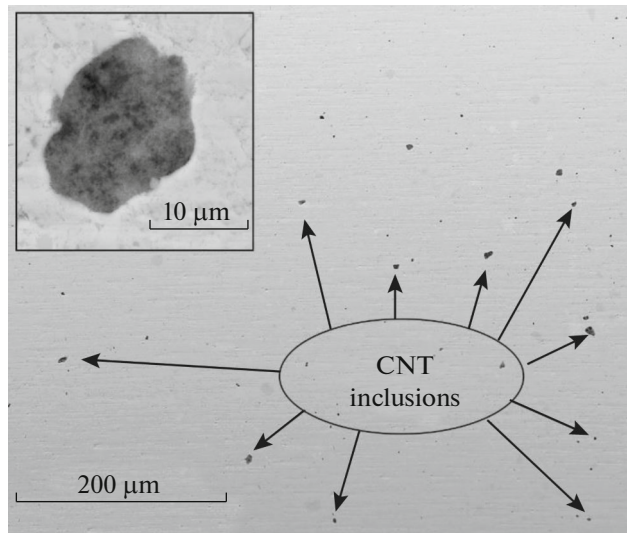


Fig. 3. EBSD image of the polished surface of the nanocomposite $\text{BiSbTe}_{1.5}\text{Se}_{1.5} + 0.5\text{-wt \% CNT}$. The inset shows a typical EBSD image of a single CNT inclusion.

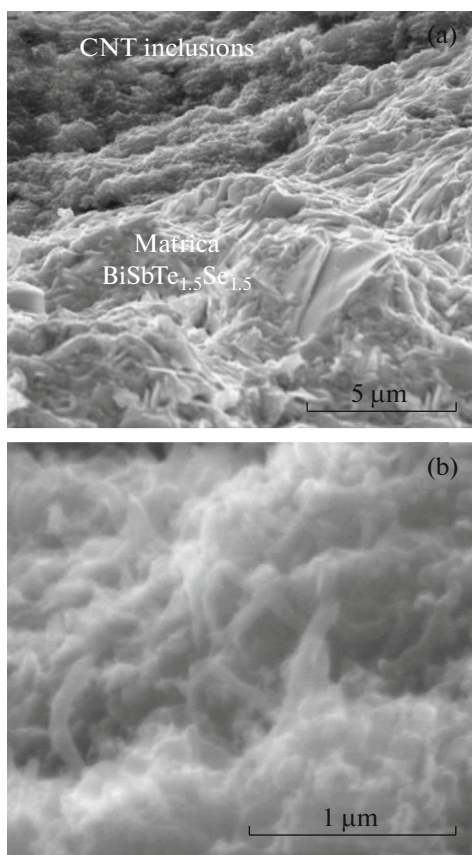


Fig. 4. SEM image of the cleavage surface of a BiSbTe_{1.5}Se_{1.5} + 0.5-wt % CNT nanocomposite (a) and internal structure of a CNT inclusion (b).

inclusions. This may be due to the high temperature evaporation of Te, which is characteristic of compounds based on bismuth telluride [12]. In polycrystalline compounds, such evaporation proceeds predominantly along the grain boundaries. In nanocomposites, apparently, Te can rapidly evaporate along the matrix/filler interfaces, which leads to its incorporation into the filler volume.

The temperature dependences of the transport properties (electrical resistivity and total thermal conductivity) of nanocomposites with different filler contents, taken in the heating mode in the range from 290 to 500 K, are shown in Figs. 6 and 7, respectively. These dependences are qualitatively similar to the corresponding dependences observed in compounds based on bismuth telluride [13–16]. The introduction of CNTs has the greatest effect on the electrical resistivity (Fig. 6). For the pure BiSbTe_{1.5}Se_{1.5} compound, the dependence $\rho(T)$ has a “metallic” character, i.e., the resistance increases with increasing temperature. This behavior is usually associated with a decrease in the mobility of electrons due to their scattering at acoustic and optical phonons [17]. However, for all BiSbTe_{1.5}Se_{1.5} + x CNT nanocomposites the character

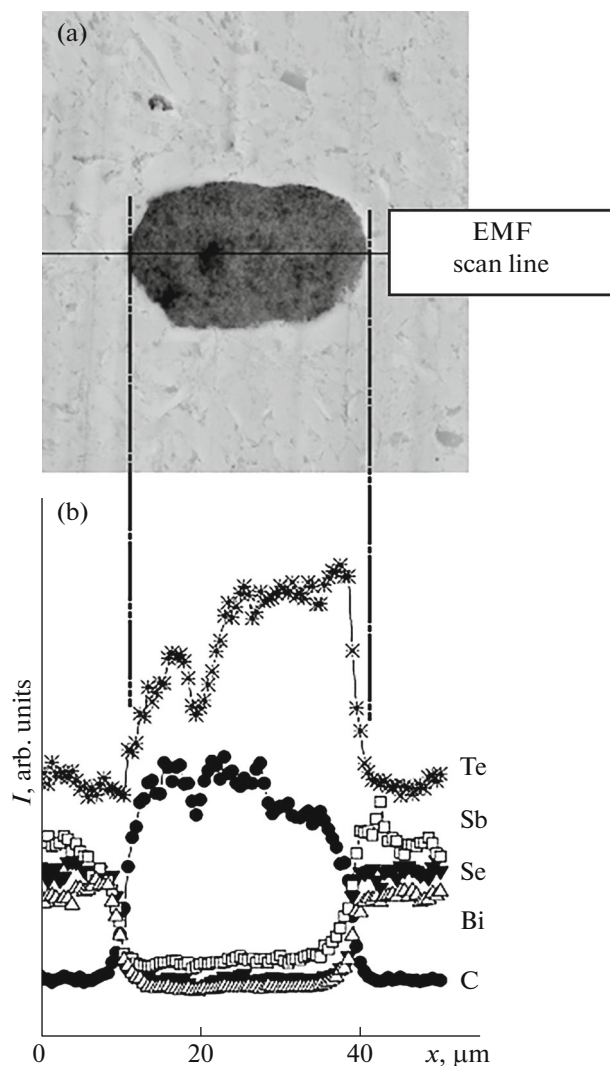


Fig. 5. EBSD image of a CNT inclusion in a BiSbTe_{1.5}Se_{1.5} + 0.5-wt % CNT nanocomposite (a); scan profiles of Bi, Sb, Te, Se, and C taken along a line crossing the inclusion (b).

of the dependence $\rho(T)$ changes from “metallic” to “semiconductor”, in which the resistance drops with increasing temperature. As a rule, in semiconductors, such a dependence is due to the thermal generation of current carriers either from the valence band to the conduction band, or from the donor (acceptor) level to the conduction band (valence band). In this case, it is necessary to assume that in nanocomposites the matrix material is alloyed with carbon during high-temperature sintering. But such a phenomenon was not observed on composites synthesized earlier from a thermoelectric matrix with a CNT filler. In addition, the study of the elemental composition did not reveal the presence of carbon in the matrix. Another mechanism of “semiconductor” behavior $\rho(T)$ in BiSbTe_{1.5}Se_{1.5} + x CNT nanocomposites can be associated with the features of their microstructure.

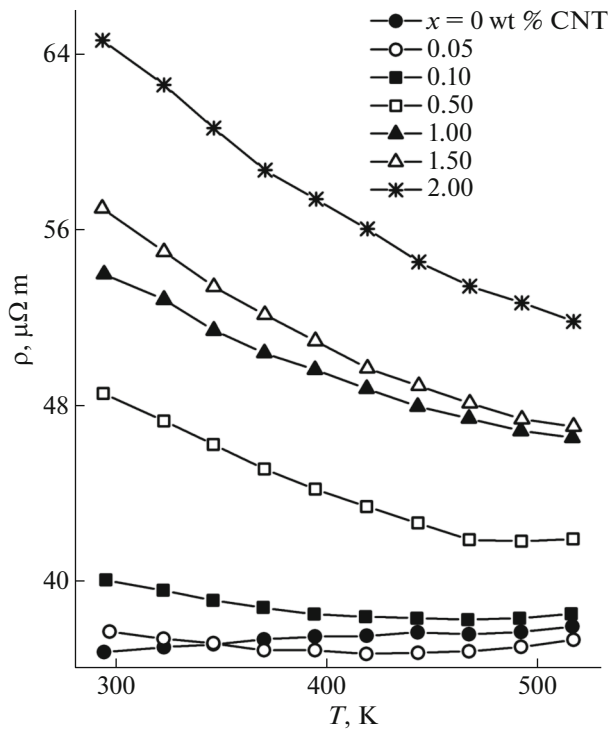


Fig. 6. Temperature dependences of the electrical resistivity of the BiSbTe_{1.5}Se_{1.5} + xCNT nanocomposite with different filler content.

Such nanocomposites are structurally inhomogeneous and consist of a matrix with filler inclusions (Figs. 3, 4). In structurally inhomogeneous solids, in which the development of structural inhomogeneity leads to the appearance of corresponding electrical inhomogeneity, the electrical resistance can decrease with increasing temperature, mimicking the true “semiconductor” behavior. In this case, current transfer will be determined by the movement of electrons through the interfaces between inhomogeneities in an inhomogeneous material. Such motion can be associated with electron tunneling through potential barriers associated with these boundaries [18–20]. As the temperature rises, the probability of overcoming the potential barrier by an electron increases, which leads to a decrease in the electrical resistance. In the studied BiSbTe_{1.5}Se_{1.5} + xCNT nanocomposites, the interfaces that electrons need to overcome correspond to the matrix/inclusion interfaces, and the number of such interfaces increases with increasing filler content.

The temperature dependences of the total thermal conductivity k for all BiSbTe_{1.5}Se_{1.5} + xCNT nanocomposites have a minimum at ~ 400 K (Fig. 7a). The appearance of this minimum is associated with a change in the mechanism of thermal conductivity. Below the minimum temperature, the main contribution to the total thermal conductivity is made by the phonon thermal conductivity k_e , at which heat transfer

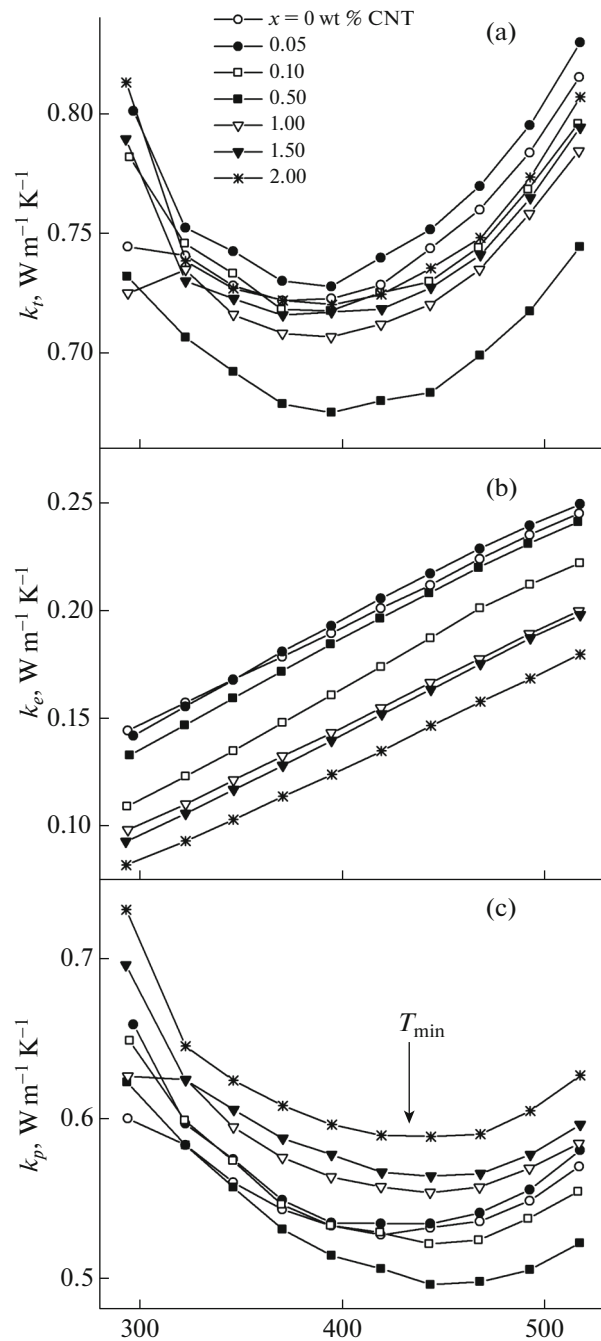


Fig. 7. Temperature dependences of the total (a), electronic (b), and phonon (c) thermal conductivity of the BiSbTe_{1.5}Se_{1.5} + xCNT nanocomposite with different filler content.

is predominantly carried out by phonons. Above the minimum temperature, the main contribution to the total thermal conductivity comes from the bipolar thermal conductivity k_b , at which heat transfer occurs as a result of the combined diffusion of electrons and holes from the heated section of the sample to the cold one, where the recombination of electron-hole pairs

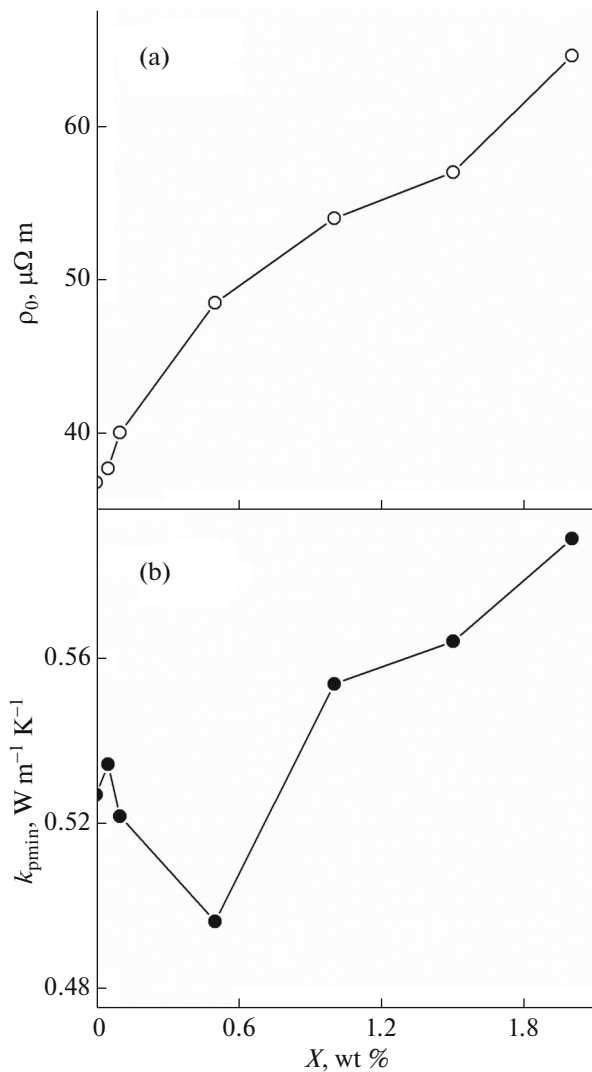


Fig. 8. Influence of the filler content in the $\text{BiSbTe}_{1.5}\text{Se}_{1.5} + x\text{CNT}$ nanocomposite on its electrical resistivity measured at room temperature (a) and the minimum value of the phonon thermal conductivity (b).

occurs with the emission of a phonon. Also, in all dependences $k(T)$ there is an electronic contribution $k_e(T)$. This contribution can be calculated using the Wiedemann–Franz law [21]:

$$k_e = \frac{LT}{\rho}, \quad (1)$$

where L is the Lorentz number.

For the $\text{BiSbTe}_{1.5}\text{Se}_{1.5}$ compound, the Lorentz number was previously defined as $1.8 \times 10^{-8} \text{ W } \Omega \text{ K}^{-2}$. This number was used to calculate the electronic contribution to the total thermal conductivity of the studied nanocomposites (Fig. 7b). All dependences $k_e(T)$ behave similarly, i.e., k_e increases almost linearly with increasing temperature. The absolute values k_e change

inversely ρ , i.e., an increase in resistance with an increase in CNT concentration leads to a corresponding decrease in the electronic contribution to thermal conductivity. The phonon contributions to the total thermal conductivity calculated as $k_p(T) = k(T) - k_e(T)$ are shown in Fig. 7c. In contrast to the electronic contribution, the phonon contribution depends on the content of CNTs in a more complex way. The minimum $k_p(T)$ at a temperature of $T_{\min} \approx 430 \text{ K}$ separates the low-temperature phonon thermal conductivity from the high-temperature bipolar thermal conductivity. Figure 8 shows the values of the minimum phonon thermal conductivity $k_{p \min}$ at a temperature of T_{\min} for the $\text{BiSbTe}_{1.5}\text{Se}_{1.5} + x\text{CNT}$ nanocomposites as a function of x . The dependence $k_{p \min}(x)$ has a minimum for the nanocomposite with $x = 0.5 \text{ wt } \%$ CNT. The extreme dependence $k_{p \min}(x)$ can be associated with the simultaneous action of at least two mechanisms of influence of inclusions on the thermal conductivity of the matrix. For nanocomposites with $x < 0.5 \text{ wt } \%$ of CNTs, the phonon thermal conductivity decreases with increasing filler content, which is due to the fact that the matrix–inclusion interfaces can effectively scatter not only electrons and increase the electrical resistance, but also phonons, which leads to a decrease in the thermal conductivity. For nanocomposites with $x > 0.5 \text{ wt } \%$ CNTs, the phonon thermal conductivity already increases, which may be due to the fact that in such nanocomposites the main contribution comes from the thermal conductivity of the material of the inclusions (their volume), rather than the matrix–inclusion interfaces. As noted above, the thermal conductivity of CNTs is high; therefore, the thermal conductivity of nanocomposites, in which the volume of inclusions with high thermal conductivity is rather large, will increase. In other words, at low filler concentrations, the phonon thermal conductivity of $\text{BiSbTe}_{1.5}\text{Se}_{1.5} + x\text{CNT}$ nanocomposites will be determined by phonon scattering at the matrix–inclusion interfaces, and at high filler concentrations, by phonon thermal conductivity of the inclusion material. Figure 8 also shows the dependence $\rho_0(x)$ (ρ_0 is the electrical-resistivity value measured at room temperature). As opposed to dependence $k_{p \min}(x)$, ρ_0 keeps growing with increasing x . This behavior is due to an increase in the number of matrix–inclusion interfaces with an increase in the filler content in nanocomposites. Thus, the effect of the CNT content on the electrical resistivity and thermal conductivity of $\text{BiSbTe}_{1.5}\text{Se}_{1.5} + x\text{CNT}$ nanocomposites turns out to be different. The obtained results suggest that the transport properties of nanocomposites can be optimized by choosing the correct filler concentration and filler-inclusion size, which will increase the thermoelectric figure of merit of nanocomposites.

CONCLUSIONS

BiSbTe_{1.5}Se_{1.5} + *x*CNT nanocomposites were obtained for the first time with different *x* = 0, 0.05, 0.1, 0.5, 1.0, 1.5, and 2.0 wt %, consisting of the medium-entropy alloy BiSbTe_{1.5}Se_{1.5} (polycrystalline matrix of the nanocomposite) and filler inclusions consisting of CNT clusters. Micron-size inclusions are randomly distributed inside the polycrystalline matrix. In the temperature range of 290–500 K, the features of their transport properties (electrical resistivity and total thermal conductivity) were studied. In contrast to the “metallic” behavior of the electrical conductivity of the BiSbTe_{1.5}Se_{1.5} matrix all nanocomposites exhibit “semiconductor” behavior. This may be due to the formation of matrix–inclusion interfaces, which electrons overcome during current transfer. The total thermal conductivity of nanocomposites depends in a complex way on the filler content. The phonon contribution to the thermal conductivity is minimal for the nanocomposite with 0.5 wt % CNT. Depending on the content of the filler, the phonon contribution can be determined either by the scattering of phonons at the matrix–inclusion interfaces, which leads to a decrease in the thermal conductivity, or by the high thermal conductivity of the CNTs of the inclusions themselves, which leads to an increase in the thermal conductivity.

FUNDING

The study was financed by the Russian Science Foundation (grant no. 21-12-00405).

REFERENCES

1. N. T. Hung, A. R. T. Nugraha, and R. Saito, *Energies* **12**, 4561 (2019).
<https://doi.org/10.3390/en12234561>
2. K. T. Kim, Y. S. Eom, and I. Son, *J. Nanomater.* **2015**, 1 (2015).
<https://doi.org/10.1155/2015/202415>
3. K. Ahmad and C. Wan, *Nanotechnologies* **28**, 415402 (2017).
<https://doi.org/10.1088/1361-6528/aa810b>
4. F. Ren, H. Wang, P. A. Menchhofer, and J. O. Kiggans, *Appl. Phys. Lett.* **103**, 221907 (2013).
<https://doi.org/10.1063/1.4834700>
5. J. Lei, D. Zhang, W. Guan, et al., *Appl. Phys. Lett.* **113**, 083901 (2018).
<https://doi.org/10.1063/1.5042265>
6. Z. Zhang, S. Wu, Y. Niu, et al., *J. Mater. Sci.: Mater. Electron.* **30**, 5177 (2019).
<https://doi.org/10.1007/s10854-019-00816-0>
7. N. Nandihalli, S. Gorsse, and H. Kleinke, *J. Solid State Chem.* **226**, 164 (2015).
<https://doi.org/10.1016/j.jssc.2015.02.016>
8. A. Schmitz, C. Schmid, J. de Boor, and E. Mueller, *J. Nanosci. Nanotechnol.* **17**, 1547 (2017).
<https://doi.org/10.1166/jnn.2017.13727>
9. A. Raphael, P. Vivekanandhan, and S. Kumaran, *Mater. Lett.* **269**, 127672 (2020).
<https://doi.org/10.1016/j.matlet.2020.127672>
10. Z. Fan, H. Wang, Y. Wu, et al., *RSC Adv.* **6**, 52164 (2016).
<https://doi.org/10.1039/C5RA28088E>
11. O. Ivanov, M. Yaprntsev, A. Vasil'ev, and E. Yaprntseva, *J. Alloys Compd.* **872**, 159743 (2021).
<https://doi.org/10.1016/j.jallcom.2021.159743>
12. F. Wu, H. Song, J. Jia, and X. Hu, *Prog. Nat. Sci. Mater. Int.* **23**, 408 (2013).
<https://doi.org/10.1016/j.pnsc.2013.06.007>
13. X. H. Ji, X. B. Zhao, Y. H. Zhang, et al., *J. Alloys Compd.* **387**, 282 (2005).
<https://doi.org/10.1088/2053-1591/aaa265>
14. J. Yang, F. Wu, Z. Zhu, et al., *J. Alloys Compd.* **619**, 401 (2015).
<https://doi.org/10.1063/1.2338885>
15. M. Yaprntsev, R. Lyubushkin, O. Soklakova, and O. Ivanov, *J. Electron. Mater.* **47**, 1362 (2018).
<https://doi.org/10.1016/j.jnsc.2013.01.003>
16. O. Ivanov, M. Yaprntsev, R. Lyubushkin, and O. Soklakova, *Scr. Mater.* **146**, 91 (2018).
<https://doi.org/10.1016/j.matchar.2014.12.001>
17. O. Ivanov and M. Yaprntsev, *Mater. Res. Express* **5**, 015905 (2018).
<https://doi.org/10.1088/2053-1591/aaa265>
18. Q. G. Zhang, X. Zhang, B. Y. Cao, et al., *Appl. Phys. Lett.* **89**, 114102 (2006).
<https://doi.org/10.1063/1.2338885>
19. H. Zeng, Y. Wu, J. Zhang, et al., *Prog. Nat. Sci. Mater. Int.* **23**, 18 (2013).
<https://doi.org/10.1016/j.pnsc.2013.01.003>
20. O. Ivanov, O. Maradudina, and R. Lyubushkin, *Mater. Charact.* **99**, 17 (2015).
<https://doi.org/10.1016/j.matchar.2014.12.001>
21. J. S. Blakemore, *Solid State Physics* (Cambridge Univ. Press, Cambridge, 1985).